Core creation in galaxies and halos via sinking massive objects

Goerdt, T ; Moore, B ; Read, J I ; Stadel, J

Abstract: We perform a detailed investigation into the disruption of central cusps via the transfer of energy from sinking massive objects. Constant density inner regions form at the radius where the enclosed mass approximately matches the mass of the infalling body. We explore parameter space using numerical simulations and give an empirical relation for the size of the resulting core within structures that have different initial cusp slopes. We find that infalling bodies always stall at the edge of these newly formed cores, experiencing no dynamical friction over many dynamical times. As applications, we consider the resulting decrease in the dark matter annihilation flux due to centrally destroyed cusps, and we present a new theory for the formation of close binary nuclei—the "stalled binary" model. We focus on one particularly interesting binary nucleus system, the dwarf spheroidal galaxy VCC 128 which is dark matter dominated at all radii. We show that its nuclei would rapidly coalesce within a few million years if it has a central dark matter cusp slope steeper than r -1. However, if its initial dark matter cusp is slightly shallower than a logslope of -0.75 at 0.1% of the virial radius, then the sinking nuclei naturally create a core equal to their observed separation and stall. This is close to the logslope measured in a recent billion particle cold dark matter halo simulation.

DOI: https://doi.org/10.1088/0004-637X/725/2/1707

Mon. Not. R. Astron. Soc. **000**, 1–10 (2008) Printed 15 March 2011 (MN LATEX style file v2.2)

Core creation in galaxies and haloes via sinking massive objects: application to binary nuclei

Tobias Goerdt[1⋆], J. I. Read[2], Ben Moore[2] and Joachim Stadel[2]

[1] *Racah Institute of Physics, The Hebrew University, Jerusalem 91904, Israel*
[2] *Institut für Theoretische Physik, Universität Zürich, Winterthurerstrasse 190, CH-8057 Zürich, Schweiz*

Draft version 15 March 2011

ABSTRACT

Massive objects sinking within galaxies or dark matter haloes via dynamical friction will exchange momentum with central particles, ejecting them from the cusp and reducing the density of the inner region. We explore parameter space using numerical simulations and give empirical relations for the size of the resulting core within structures that have different initial cusp slopes. We show that simple energetic arguments can be used to predict these scaling laws. As an application we consider the dwarf spheroidal galaxy VCC 128 which has a double nucleus separated by less than a hundred parsecs. If this galaxy has a surrounding cold dark matter halo with central density proportional to r^{-1} then these objects should sink to the centre of the cusp and coalesce in a few million years. We show that the sinking nuclei naturally create a core equal to their current separation if the initial dark matter cusp is slightly shallower than a log slope of -0.75 at $\sim 0.1\%$ of the virial radius. The sinking objects naturally stall at this radius for many Gyrs. This may be indirect observational evidence for central dark matter cusps shallower than r^{-1} at the very centres of dark matter haloes.

Key words: cosmology: theory – dark matter – galaxies: dwarf – galaxies: individual: VCC 128 – methods: numerical

1 INTRODUCTION

Massive objects orbiting within a cuspy mass distribution are expected to lose momentum and sink via dynamical friction (Chandrasekhar 1943; White 1983; Hernquist & Weinberg 1989; Capuzzo-Dolcetta & Vicari 2005). While spiralling inwards the massive perturber transfers momentum to central particles/stars etc, moving them to a larger orbital radius. One proposed effect of this process is to make a primordially cuspy dark matter distribution shallower (El-Zant, Shlosman & Hoffman 2001; Tonini, Lapi & Salucci 2006).

In the prevailing ΛCDM cosmology primordial dark matter haloes are cuspy, having an inner density slope $\rho(r) \propto r^{-\gamma}$ with $\gamma > 1$ beyond $\approx 1\%$ of the virial radius (Dubinski & Carlberg 1991; Diemand, Moore & Stadel 2005). By contrast, observations of dwarf galaxies seem to indicate that they have a cored mass distribution (Sánchez-Salcedo, Reyes-Iturbide & Hernandez 2006; Goerdt et al. 2006; Kleyna et al. 2003), while controversial evidence for cored mass distributions in dwarf spiral galaxies has been debated for over a decade (Moore 1994).

A sufficiently compact sinking perturber will transform an initially cuspy host halo into a cored one on some scale. Once a core has formed then dynamical friction is no longer effective (Goerdt et al. 2006). Dynamical arguments show that sinking perturbers must stall at the outer edge of a core (Read et al. 2006).

Here we quantify this stalling behaviour as a function of perturber mass $M_{\rm pert}$ and central cusp slope γ. We consider a much larger range in $M_{\rm pert}$ and γ than in previous papers (Goerdt et al. 2006; Read et al. 2006) and find that stalling persists even at very high perturber mass, as found also recently by Gualandris & Merritt (2008). We fit empirical scaling relations using high resolution N-body simulations and attempt to explain these using simple energetic arguments. As an example we attempt to explain the close separation of binary nuclei within the Virgo cluster dwarf galaxy VCC 128 (Debattista et al. 2006). We show that the two nuclei are expected to sink into the centre of a cuspy halo, and coalesce there on timescales which are extremely short compared to the age of the galaxy. We will discuss

⋆ tgoerdt@phys.huji.ac.il

Halo	γ	ρ_0 / $M_\odot pc^{-3}$	r_s/ kpc	con	M_{vir} / $M_\odot$
A	1.75	0.000232	20.8	3.88	3.10×10^{10}
B	1.50	0.001333	10.3	7.50	2.71×10^{10}
C	1.00	0.009109	5.01	15.0	2.50×10^{10}
D	0.75	0.017732	3.91	19.0	2.43×10^{10}
E	0.50	0.027746	3.38	22.0	2.40×10^{10}

Table 1. The parameter list of the five different dark matter haloes, we use in our analytical and numerical calculations.

further applications to multiple nuclei seen in galaxies like Andromeda and in cluster cD galaxies in future work.

This paper is organised as follows: In §2 we describe our analytical framework, which is supported using N-body simulations. In §3 we apply our findings to VCC 128 and in §4 we give our conclusions.

2 TRANSFORMING CUSPS TO CORES

We use the split-power law α, β, γ model for our initial background distribution (Hernquist 1990; Saha 1992; Zhao 1996):

$$\rho(r) = \frac{\rho_0}{(r/r_s)^\gamma \left[1 + (r/r_s)^\alpha\right]^{(\beta-\gamma)/\alpha}} \qquad (r \leqslant R_{vir}) \qquad (1)$$

where ρ_0 and r_s are the central density and scale length respectively, γ is the inner log slope, α is the log slope at the 'knee' of the profile, and β is the outer log slope. Since we focus on the very inner regions of the halo in our analysis, α and β are not critical. We fix them at the commonly accepted values for cold dark matter haloes of 1 and 3, respectively.

We will take our fiducial model to represent a low mass dark matter halo typical of those surrounding dwarf galaxies with a maximum circular velocity $v_{peak} = 50$ km s^{-1}. As our application later, we will consider the Virgo cluster dwarf galaxy VCC 128 which has an absolute bolometric luminosity of $M_B = -15.5$ mag (Debattista et al. 2006). We estimate its maximum circular velocity to be $v_{peak} =$ 35 - 65 km s^{-1} using the Faber-Jackson relation of dEs (de Rijcke et al. 2005). Assuming a concentration of 15 for $\gamma = 1.0$, which is a common value for cosmologically motivated dwarf spheroidals (Łokas 2002), we get a $r(v_{peak})$ of 10.75 kpc. For our other models we keep v_{peak} as well as $r(v_{peak})$ constant, just varying γ. This leads to the parameters given in Table 1 and to the circular velocity curves and radial density profiles, which are shown in Fig. 1.

With the above assumptions, VCC 128 is likely dark matter dominated at all radii. We estimate its stellar mass distribution in two different ways. Firstly, we use the Sersíc profile parameters derived in Debattista et al. (2006) normalised to give a total luminosity in the B-band of $M_B = -15.5$ mag:

$$\Sigma(R) = \Upsilon_B I_e \exp\left\{-b_n\left[\left(\frac{R}{R_e}\right)^{\frac{1}{n}} - 1\right]\right\} \qquad (2)$$

with $b_n = 1.9992n - 0.3271$ (Graham & Driver 2005), $n = 0.55$, $R_e = 14.5$ arcsec and assuming a B-band mass to light ratio $\Upsilon_B = 3$ for dE galaxies as in Read & Trentham (2005). We then de-project the stellar mass distribution using the usual Abel integral equation (that assumes spherical symmetry):

$$\rho(r) = -\frac{1}{\pi}\int_r^\infty \frac{d\Sigma(R)}{dR}\frac{dR}{\sqrt{R^2 - r^2}}. \qquad (3)$$

The resulting density and cumulative mass distributions are given by the solid lines in Fig. 1. Secondly, we use the stellar masses derived from fits to the spectral energy distribution (SED) of the galaxy nucleus and the whole galaxy as given in Debattista et al. (2006). These are overlaid on the right panel of Fig. 1 (crosses) and give an excellent match to the cumulative mass distribution derived from the Sersíc fit to the light profile. We assume from here on that the dark matter is dynamically dominant and that the stars are to a good approximation a massless tracer population.

2.1 Analytical model

Previously published work has demonstrated numerically (El-Zant, Shlosman & Hoffman 2001; Read et al. 2006) and semi-analytically (Tonini, Lapi & Salucci 2006) that a sinking massive compact object – a *perturber* – will transfer energy and angular momentum to the background via dynamical friction, creating a central constant density core from an initially cuspy density distribution. Here, we calculate analytically how the size of this core will scale for a given initial background density distribution and perturber mass.

The dynamical friction sinking timescale of the perturber can be derived using the Chandrasekhar dynamical friction formula (Chandrasekhar 1943). Assuming that the perturber is always on a circular orbit, and that the background particles have a Maxwellian velocity distribution, we can calculate the infall rate:

$$\frac{dr}{dt} = -\frac{4\pi \ln\Lambda(r)\rho(r)G^2 M_{pert} r}{v_c^2(r)\mathrm{d}\left[r v_c(r)\right]/\mathrm{d}r}\left\{\mathrm{erf}\left[\frac{v_c(r)}{\sqrt{2}\sigma(r)}\right] - \frac{2v_c(r)}{\sqrt{2\pi}\sigma(r)}\exp\left[\frac{-v_c^2(r)}{2\sigma^2(r)}\right]\right\}, \qquad (4)$$

where $v_c(r)$ is the circular speed at radius r; M_{pert} is the mass of the in-falling body; $\ln\Lambda(r)$ is the Coulomb logarithm [$\Lambda = b_{max}/b_{min}$]; $\rho(r)$ is the density of the dark matter halo at radius r according to equation (1); and $\sigma(r)$ is the one-dimensional velocity dispersion of the halo.

Equation (4) assumes that dynamical friction is a local process that proceeds by local momentum exchange between the perturber and the background. This cannot be the whole story. Firstly, it implies that if $\rho(r) \to 0$ there will be no dynamical friction. Secondly, it implies that if $\rho(r) \to$ const, nothing special should happen and dynamical friction should proceed as for any other $\rho(r)$. Both of these statements conflict with numerical results (Lin & Tremaine 1983; Tremaine & Weinberg 1984; Colpi, Mayer & Governato 1999; Goerdt et al. 2006; Read et al. 2006). The implication is that dynamical friction is not a local process, but rather is driven by global resonances (Tremaine & Weinberg 1984; Read et al. 2006). In the former case, resonances (and therefore friction) are present even outside of a galaxy where $\rho(r) = 0$. In the latter case, $\rho =$ const. is a harmonic potential which is especially resonant. This allows the perturber and the back-

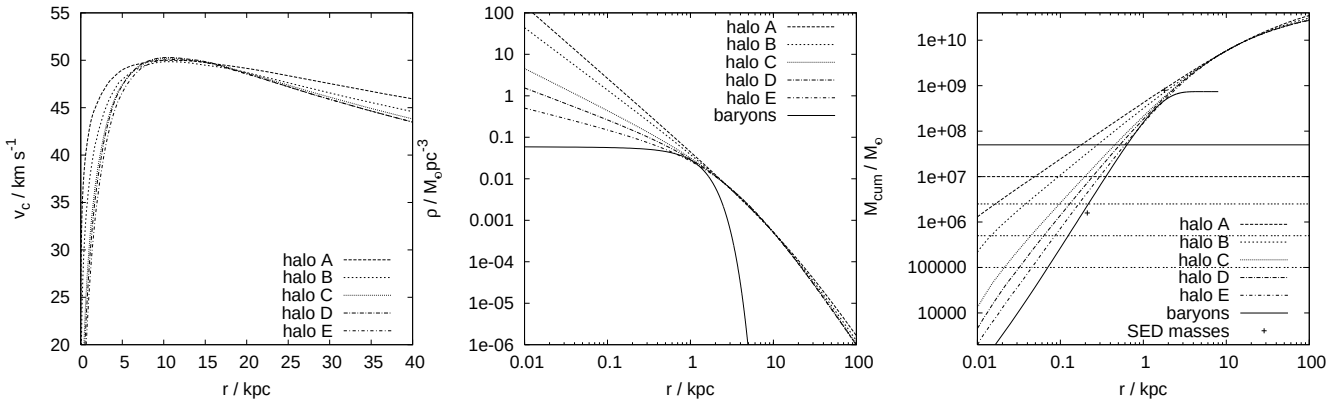

Figure 1. Circular velocities (*left*) radial density profiles (*middle*) and cumulative mass (*right*) for haloes A, B, C, D, E. All five of them peak at 50 km s^{-1} at 10.75 kpc. The horizontal lines on the right panel show the perturber masses $M_{\rm pert}$ we use in the simulations (§2.2). The solid lines and the crosses show estimates of the baryonic (stellar) mass distribution of the dSph galaxy VCC 128.

ground reach a stable state with no net momentum exchange (Kalnajs 1972; Read et al. 2006).

Despite the above difficulties, in most situations, equation (4) works remarkably well. This is because the non-local effects enter only logarithmically through $\ln\Lambda$. We use this fact in our calculation, below. We assume that the perturber transfers all of its energy and angular momentum locally in a spherical shell. Provided that we are not in the regime where the local density tends to zero, or the background and the perturber are especially resonant this will be a good approximation.

Equation (4) assumes the perturber starts and remains on a circular orbit. As a result, the energy transferred to the background particles in moving from radius $r+\delta r$ to r does not depend on the dynamical friction process itself. All we need to know is that the perturber moves inwards from one circular orbit to the next. In this case, we have:

$$\begin{aligned}\delta E_{\rm trans} &= \frac{\rm d}{{\rm d}r}\left[\frac{1}{2}M_{\rm pert}v_{\rm c}^2 + M_{\rm pert}\Phi(r)\right]\delta r \\ &= M_{\rm pert}\left[\frac{G}{2r}\frac{{\rm d}M(r)}{{\rm d}r} - \frac{GM(r)}{2r^2} + \frac{{\rm d}\Phi(r)}{{\rm d}r}\right]\delta r \quad (5)\end{aligned}$$

where $M(r)$ is the mass of background particles enclosed at radius r. We assume that this energy is injected into background particles contained within a spherical shell about the perturber. These gain specific energy ΔE given by:

$$4\pi\rho r^2\delta r\Delta E = \delta E_{\rm trans} \quad (6)$$

and rearranging gives:

$$\Delta E = \frac{M_{\rm pert}}{4\pi\rho r^2}\left[\frac{G}{2r}\frac{{\rm d}M(r)}{{\rm d}r} - \frac{GM(r)}{2r^2} + \frac{{\rm d}\Phi(r)}{{\rm d}r}\right] \quad (7)$$

We may solve equation (7) exactly if we specify the distribution of background particles. A particularly useful choice is the split power law models given by equation (1) with $\alpha = 1$ and $\beta = 4$:

$$\rho(r) = \frac{M_{\rm t}(3-\gamma)}{4\pi r_{\rm s}^3}\left(\frac{r}{r_{\rm s}}\right)^{-\gamma}\left(1+\frac{r}{r_{\rm s}}\right)^{\gamma-4} \quad (8)$$

$$M(r) = M_{\rm t}\left(\frac{r}{r_{\rm s}}\right)^{3-\gamma}\left(1+\frac{r}{r_{\rm s}}\right)^{\gamma-3} \quad (9)$$

$$\Phi(r) = \frac{GM_{\rm t}}{r_{\rm s}(2-\gamma)}\left[\left(1+\frac{r_{\rm s}}{r}\right)^{\gamma-2} - 1\right] \quad (10)$$

Where $M_{\rm t}$ is the total mass, $r_{\rm s}$ is the scale length, and γ is the central log density slope. This gives:

$$\Delta E = \frac{GM_{\rm pert}}{2(3-\gamma)r}\left(4-\gamma+\frac{r}{r_{\rm s}}\right) \quad (11)$$

We assume that this energy is injected over one dynamical time and that the system then rearranges itself on a timescale longer than this. In this impulse approximation, prior to rearrangement, the potential $\Phi(r)$ remains constant, while the specific kinetic energy of the background increases from $T_{\rm i} \rightarrow T_f$. We can obtain an estimate of $T_{\rm i}$ if we assume that all of the background particles move on circular orbits:

$$T_{\rm i}(r) = \frac{v_{\rm c}^2}{2} = \frac{GM_{\rm t}}{2r}\left(\frac{r}{r_{\rm s}}\right)^{3-\gamma}\left(1+\frac{r}{r_{\rm s}}\right)^{\gamma-3} \quad (12)$$

Now, if we write:

$$\frac{T_{\rm f}(r) - T_{\rm i}(r)}{T_{\rm i}(r)} = \kappa \quad (13)$$

Then the radius at which $\kappa \sim 1$ is the radius at which the background specific kinetic energy doubles.

After the above energy injection, the system must then return to virial equilibrium. Assuming no mass escapes during this phase, the specific kinetic energy must be converted to potential energy and the system will expand. The maximal effect leads to a constant density core since density cannot decrease inwards for a stable system. We assume that the radius of this core $r_{\rm c}$ is related to the radius at which the specific kinetic energy doubles. Combining equations (11), (12) and (13) and assuming $r_{\rm c} \ll r_{\rm s}$, we obtain for $r_{\rm c}$:

$$\frac{r_{\rm c}}{r_{\rm s}} \simeq \left(\frac{M_{\rm pert}}{M_{\rm t}}\frac{4-\gamma}{3-\gamma}\frac{1}{\kappa}\right)^{\frac{1}{3-\gamma}} \quad (14)$$

Where κ remains as a fitting parameter. We find $\kappa = [13.32, 2.192, 0.441, 0.224, 0.167]$ provides a good fit for haloes A, B, C, D, E to the simulations presented in §2.2.

Note that we have not considered the angular momentum imparted to the background by the perturber. This may be calculated similarly to the above and is important for determining the final orbit structure (Tonini, Lapi & Salucci

2006), but not the above scaling relations. Note also that very similar scaling to that in equation (14) may be obtained by simply comparing the enclosed mass within $r_{\rm c}$ with the mass of the perturber. Taking $M_{\rm pert} \sim M(r_{\rm c})$ and assuming $r_{\rm c} \ll r_{\rm s}$, we have $r_{\rm c}/r_{\rm s} \propto (M_{\rm pert}/M_{\rm t})^{1/(3-\gamma)}$. However, as demonstrated in Read et al. (2006), the stalling behaviour that occurs when $\rho \sim$ const. is not simply the result of $M_{\rm pert} \sim M(r_{\rm c})$. For large cores, stalling occurs even when this criteria is not met. Finally, note that $r_{\rm c}$ does not depend on the initial radius of the perturber, only on $M_{\rm pert}$ and the distribution of the background.

Our result agrees well with previous studies. El-Zant, Shlosman & Hoffman (2001) use a semianalytical Monte Carlo approach based on the Chandrasekhar approximation to estimate core sizes. They let $100 - 500$ perturbers, which have a combined mass of 10% of the host halo, sink into a $\gamma = 1.0$ halo. They find $r_{\rm c} \approx r_{\rm s}$. Putting $M_{\rm pert}/M_{\rm t} = 0.1$ into equation (14) we find, using $\kappa = 0.441$ for a $\gamma = 1.0$ halo, $r_{\rm c} = 0.58 r_{\rm s}$. Goerdt et al. (2008) let 10 live globular clusters, which have a combined mass of 0.28% of the host halo, sink into a $\gamma = 1.0$ halo. They do not measure the core size explicitly but in their Fig. 1 the initial dark and the final dark lines depart at around 200 pc. Putting $M_{\rm pert}/M_{\rm t} = 0.0028$ into equation (14) we find, using $\kappa = 0.441$, $r_{\rm c} = 150$ pc. Given the uncertainty on κ, our estimates agree very well with what has already been published in the literature.

2.2 N-body simulations

In this section, we perform N-body simulations with the haloes A, B, C, D, E presented in Table 1 to study the effects of different mass perturbers on modifying the density profiles. Equilibrium N-body representations of these haloes were created with the algorithm described in Kazantzidis, Magorrian & Moore (2004) using the multimass technique of Zemp et al. (2008). This gives structures that have an effective resolution in the region of interest equivalent to using $\sim 10^{10}$ single mass particles. We ran a grid of simulations with $M_{\rm pert} = [10^5, 5 \times 10^5, 2.5 \times 10^6, 10^7, 5 \times 10^7]\,{\rm M}_\odot$ for each of the haloes A, B, C, D, E corresponding to varying the initial central log density slope: $\gamma = [1.75, 1.5, 1, 0.75, 0.5]$ (see Table 1). The perturbers were typically started at a radius of 0.4 kpc, except for the heaviest perturbers which we had to start further out for reasons which will be explained in §2.2.1. (We could have started all nuclei at the outermost radius and obtained the same results, but this would have produced avoidable computational costs. See Fig. 5.) All simulations are shown using circular orbits but similar scaling laws were found using more eccentric orbits. The resulting trajectories are given in Figure 2 and the resulting stalling radii in Figure 3.

2.2.1 Kickback and stall

For all trajectories there is a kickback which occurs after a first point of closest approach (fpca). The perturber moves away for a while, reaches a maximum, and then returns to a second point of closest approach (spca), where it finally stalls. The distance of the perturber from the centre of the halo is the same up to the noise level at fpca and at spca. We define the height of the kickback to be the difference between the lowest and the highest point during the kickback period. It is interesting that the local minima to the right and to the left of the kickback, fpca and spca, are approximately equal in height.

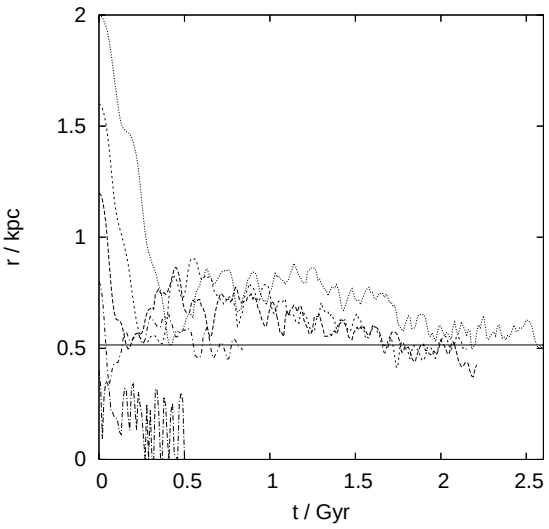

Figure 5. Simulated position of a single perturber with identical mass (5×10^7 ${\rm M}_\odot$) but different initial radii within halo D as a function of time. The stalling radius is indicated by the solid line.

The kickback occurs at $\sim r_{\rm c}$ because $M_{\rm pert} \simeq M(r_{\rm c})$ (see §2.1). At this point, the acceleration on the perturber due to the background is equal to the acceleration on the background due to the perturber, and the centre of mass of the system is significantly displaced. The background, unlike the perturber, however is not solid and rapidly rearranges itself to form the central constant density core, after which the perturber stalls. We assume that the duration of the kickback is proportional to the crossing time within the core $t_{\rm kickback} = \chi t_{\rm cross}$, which gives:

$$t_{\rm kickback} = \chi \frac{r_{\rm c}}{v_{\rm c}\,(r_{\rm c})}. \tag{15}$$

Using equations (9), (14) and assuming $r_{\rm c} \ll r_{\rm s}$, this gives:

$$t_{\rm kickback} = \chi \sqrt{\frac{r_s^3}{GM_t}} \left[\frac{M_p}{M_t} \frac{4-\gamma}{3-\gamma} \frac{1}{\kappa} \right]^{\frac{\gamma}{6-2\gamma}} \tag{16}$$

The height of the kickback may then be estimated as:

$$h_{\rm kickback} = t_{\rm kickback} v_{\rm c}(r_{\rm c}) = \phi r_{\rm c} \tag{17}$$

The duration and height of the kickback as a function of $M_{\rm pert}$ are given in Fig. 4 . We find $\chi = 80.56$ and $\phi = 0.5587$ provide good fits.

In Fig. 5, we show the stalling radius $r_{\rm c}$ as a function of the initial radius $r_{\rm i}$. As expected from the analytic calculation in §2.1, $r_{\rm c}$ does not depend on $r_{\rm i}$ as long as $r_{\rm i} > r_{\rm c}$. Only the simulation which starts with $r_{\rm i} < r_{\rm c}$ stalls well inside $r_{\rm c}$. Since all of the simulations had to be started outside of $r_{\rm c}$, the very heavy perturbers had to be started further out than the light perturbers. This does not affect any of the results, presented here. Both the height and the duration of the kickback are independent of the initial radius as well, in

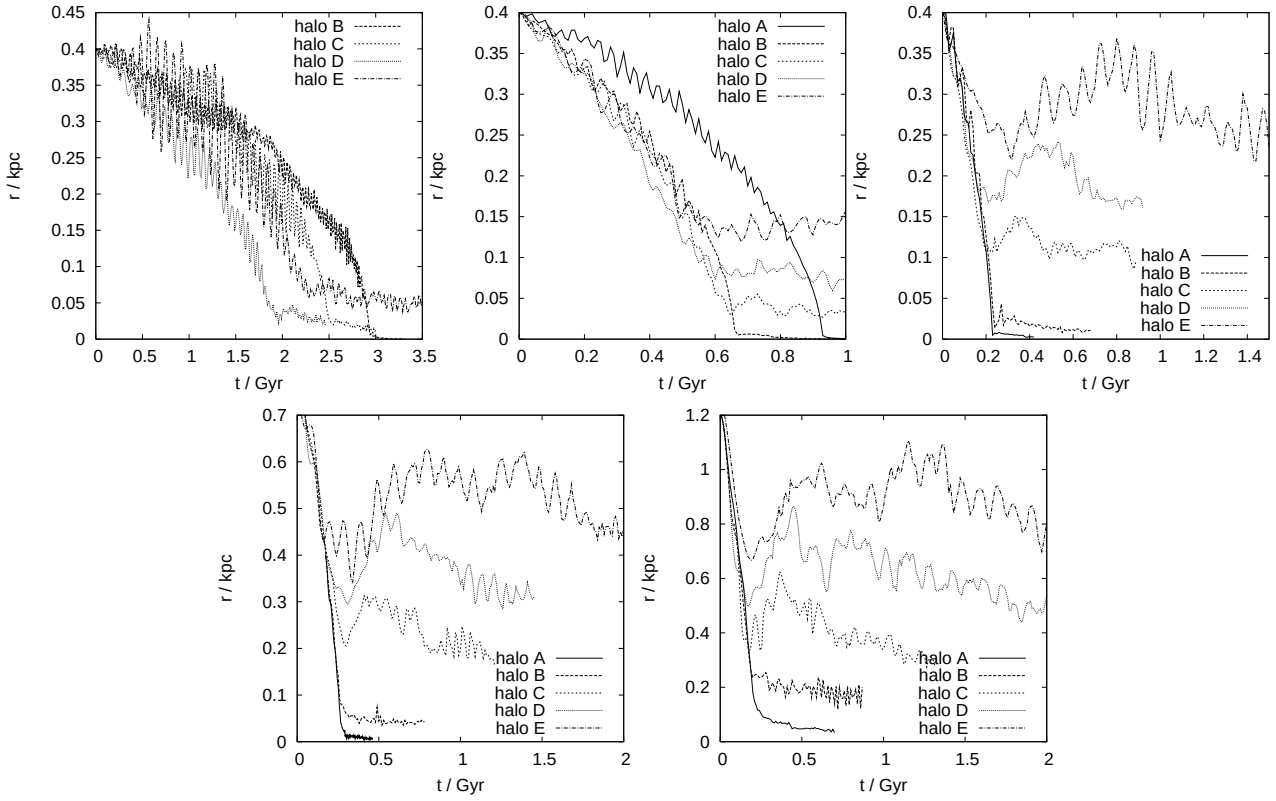

Figure 2. Simulated position of a single perturber within varying haloes. From left to right upper panels show perturber mass $M_{\rm pert} = [10^5, 5 \times 10^5, 2.5 \times 10^6]\,{\rm M}_\odot$ and lower panels mass $M_{\rm pert} = [10^7, 5 \times 10^7]\,{\rm M}_\odot$.

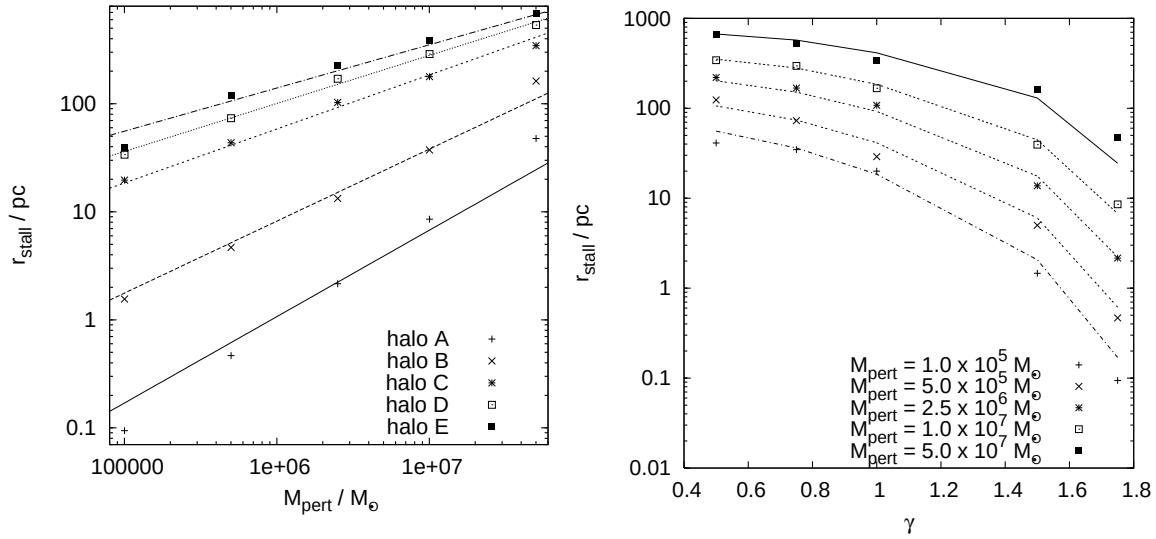

Figure 3. The stalling radii as a function of $M_{\rm pert}$ for varying γ (*left*) and as a function of γ for varying $M_{\rm pert}$ (*right*). Analytic models are also shown.

the sense that there is no monotonic relation between $r_{\rm i}$ and either the height or the duration of the kickback.

2.2.2 Core creation

The density profiles of the respective host halo at fpca and at spca are plotted in Fig. 6 and Fig. 7. One can clearly see that the density distribution changes significantly. The haloes settle down into a new equilibrium between fpca and

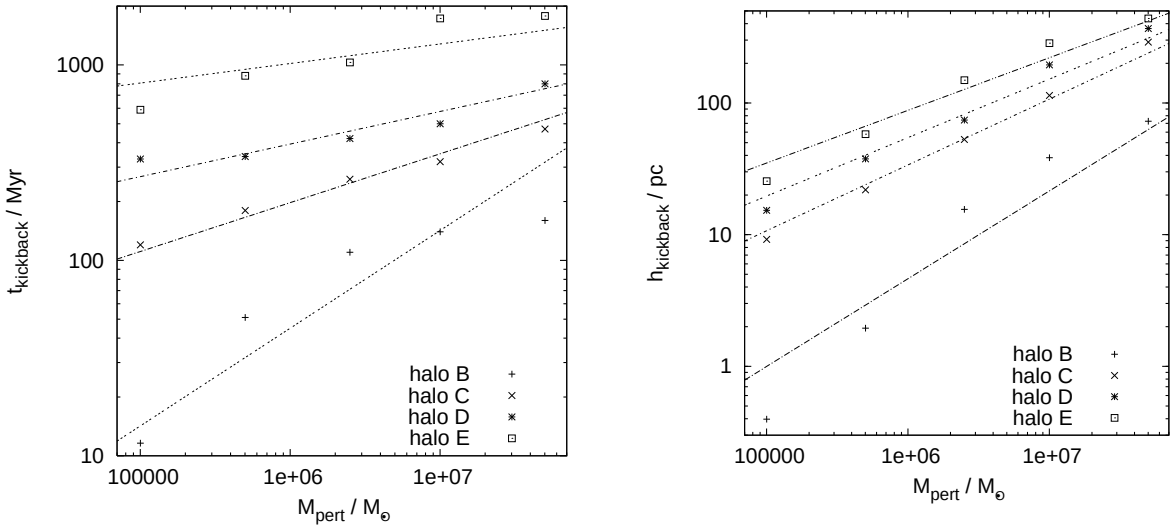

Figure 4. Duration (*left*) and height (*right*) of the kickback as a function of $M_{\rm pert}$ for haloes B, C, D, E, together with our analytic models. We do not show halo A on these plots because the data were too noisy to give reliable data points.

spca. The radial density profiles change from being cuspy to having a core: as the perturber mass increases the initial cusp is gradually flattened to a systematically higher degree until a constant density core is attained. Note that our previous analytic estimates give an estimate as to the radius within which the density profile is affected by the perturber.

The change from cuspy to cored central density is important for the expected annihilation signal from a weakly interactive massive (WIMP) dark matter particle, since the annihilation signal goes as the density squared. The net flux coming from WIMP annihilation is given by (e.g, Koushiappas 2006; Goerdt et al. 2007):

$$F = k \int_{\rm r_{min}}^{\infty} 4\pi r^2 \rho(r)^2 {\rm d}r \qquad (18)$$

where the dependence of the flux on the WIMP mass and interaction cross section is wrapped up inside the constant k. The lower bound $r_{\rm min}$ is defined as the central region of the host halo in which the neutralinos have already annihilated. The required number density for this to happen can be estimated using:

$$t_{\rm h} = \frac{1}{n\sigma v} \qquad (19)$$

where $t_{\rm h} \approx 13$ Gyrs is the Hubble time, $\sigma v \approx 10^{-30}$ cm^{3}s^{-1} is a typical cross section and n is the number density of neutralinos. For more details see Calcáneo-Roldán & Moore (1999). The minimum radius can now be computed (for a sinking perturber of a given mass) by comparing this minimum number density with the density profile in Fig. 7. Assuming a WIMP mass of 100 GeV and deploying the above mentioned density profile, $r_{\rm min}$ is of order 10^{-14} pc. Fig. 8 shows the resulting annihilation flux. It is more or less independent of the assumed WIMP mass, because this mass only goes into the calculation of $r_{\rm min}$, which is very small. For typical core sizes of $r_c \simeq 0.1 r_s$, core creation can lead to a decrease in flux of up to a third. A much weaker effect would result from a single sinking star; for example a $10 M_\odot$ star would creating a core of radius 0.34pc in our fiducial halo.

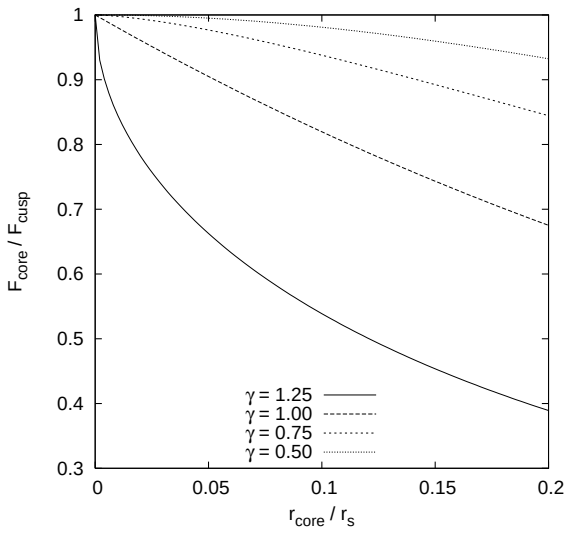

Figure 8. The flux of annihilation products from different host haloes after the central cusp core transformation relative to the untransformed initial cusp. Typical core sizes ($r_{\rm c} \approx 0.1 r_{\rm s}$) can lead to a decrease in flux of up to one third. The solid line shows $\gamma = 1.25$ and is not related to any of the haloes used throughout the rest of the paper (the corresponding values for $\gamma \geqslant 1.5$ diverge).

3 APPLICATION TO VCC 128

In this section, we apply our results to VCC 128, a dwarf spheroidal galaxy (dSph) at the outskirts of the Virgo cluster. A very close binary nucleus has recently been discovered there (Debattista et al. 2006). The two nuclei are very similar in their appearance with masses estimated to be around

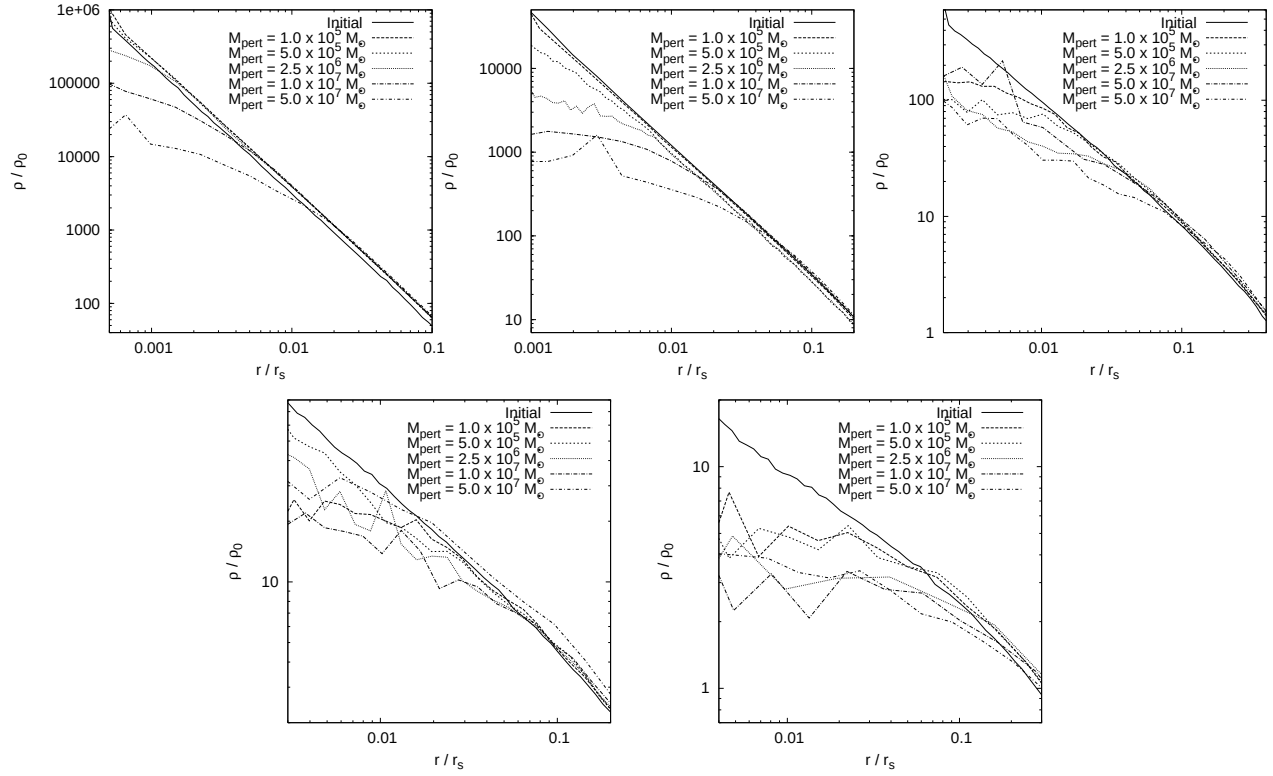

Figure 6. Density profiles of the host halo at fpca for the different nuclei masses $M_{\rm pert}$. From left to right upper panels show haloes A, B, C and lower panels haloes D and E.

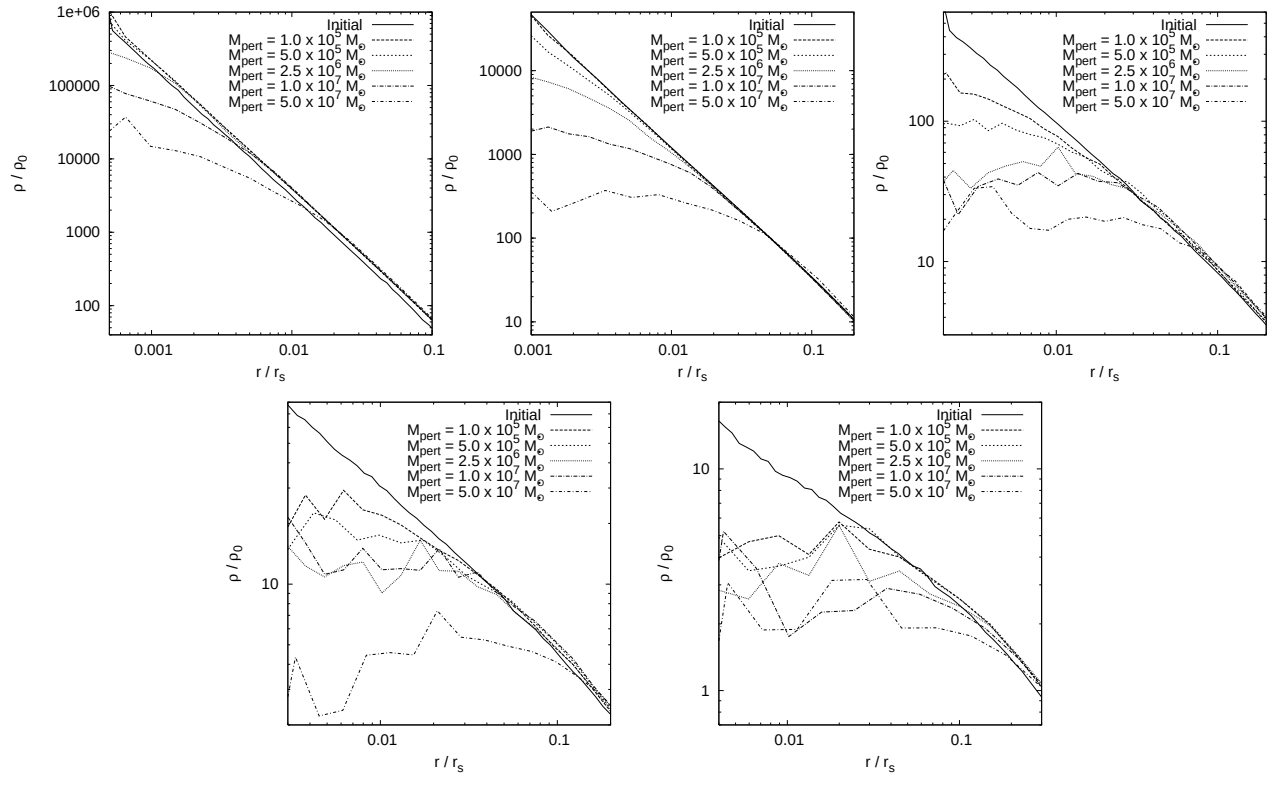

Figure 7. Density profiles of the host halo at spca for the different nuclei masses $M_{\rm pert}$. From left to right upper panels show haloes A, B, C and lower panels haloes D and E.

5×10^5 $M_\odot$. These authors found altogether 3 dSph galaxies with double nuclei, looking at HST archival images of 50 dwarf spheroidals from a survey by Lotz, Miller & Ferguson (2004). The projected distance of the two nuclei in VCC 128 is 32 pc. Debattista et al. (2006) suggest, because the two nuclei have very similar colours and magnitudes that this could be evidence for a nuclear disc around a supermassive black hole (SMBH), a situation as in NGC4486B (Lauer et al. 1996) and similar to the one in M31 (Tremaine 1995). However, it is not confirmed that such an SMBH can exist in a dwarf galaxy like VCC 128. Ferrarese (2002) found from a sample of 36 galaxies, tentative evidence that SMBH formation becomes inefficient in haloes below a dynamical mass of $\sim 5 \times 10^{11}$ $M_\odot$, though more recent work may suggest otherwise (Ferrarese et al. 2006; Wehner & Harris 2006). As such, it is interesting to explore alternative explanations.

Figure 9 shows the time taken for two nuclei that have masses $5 \times 10^5\,M_\odot$ and initial separation of 44 pc to sink via dynamical friction in halos B,C,D and E, assuming that equation 4 fully describes the friction process. In all haloes with cusp slopes shallower than 0.75, the nuclei coalesce rapidly. This suggests that, were equation 4 the whole story, it would be very unlikely to observe 3 close nuclei out of 50 dSph galaxies in Virgo. However, as we have demonstrated in the previous section, the merging nuclei will create a small core and stall indefinitely, leading to a much higher probability of observing double nuclei. We quantify this in detail below.

We assume that all dwarf galaxies for which no double nuclei have been observed: (a) do not have double nuclei at their centres; (b) lost their double nuclei because of a sink-in process due to dynamical friction, and that all dwarf galaxies, for which double nuclei actually have been observed; and (c) have double nuclei as close as the ones in VCC 128 (this assumption is made not only for the sake of numerical convenience, but also because of lack of precise observational measurements). It is important to note that there are uncertainties in these assumptions: Out of the 47 dwarf ellipticals, which do not have double nuclei, there might be some which actually do have such nuclei but the latter are too close to each other to be observed. Moreover, not all dwarf galaxies necessarily developed double nuclei during their lifetime.

Throughout this section we will assume that out of two orbiting nuclei one sinks to the centre of the underlying dark matter distribution and the other one is orbiting it afterwards. So we interpret the distance between the two nuclei as the distance of one nucleus to the centre of the dark matter distribution. We performed several N-body simulations to verify that this assumption holds.

Using equation (4), we can calculate the time it would take for one of the nuclei to sink to the centre of the system. In all our calculations we assume a constant Coulomb logarithm $\ln \Lambda(r) = 4.0$ (see Peñarrubia, Just & Kroupa 2004, for a detailed discussion of $\ln \Lambda$ varying with r). We assume that the vector connecting the two nuclei has a random orientation. We define inclination in a way that it is equal to 0° if there is a right angle between the line of sight and this vector. The probability density of its inclination is $\Psi(i) = \cos(i)$. From this, it follows that in $P_{\rm angle} = 70\%$ of the cases the inclination is lower than 43° or the de-projected distance between the nuclei is lower than 44 pc. To make a start, we will use this value as the true distance. For halo B the total sink-in time is computed to be 7.4 Myr, Halo C's sink-in-time is 13.9 Myr, Halo D's sink-in time is 38.1 Myr and Halo E's sink-in time is 171 Myr. The sink-in behaviour of the nuclei for all four cases can be seen in Fig. 9. We assume that the current age of the galaxy is 10.0 Gyr. So the time it takes for the two nuclei to coalesce is about 0.075%, 0.14%, 0.38% and 1.7% of the lifetime of the galaxy, respectively. This means that it would be highly improbable to observe binary nuclei in the present. We want to elaborate a bit further on the comparison of these probabilities. The sample we are working with has 50 galaxies in total, out of which 3 have double nuclei. When we look at one random galaxy at a random time for halo D, the probability of seeing a double nucleus is $P_{\rm dn} = 0.0038$. The probability of seeing more than 2 galaxies with double nuclei in a sample of 50 is given by the cumulative binomial distribution:

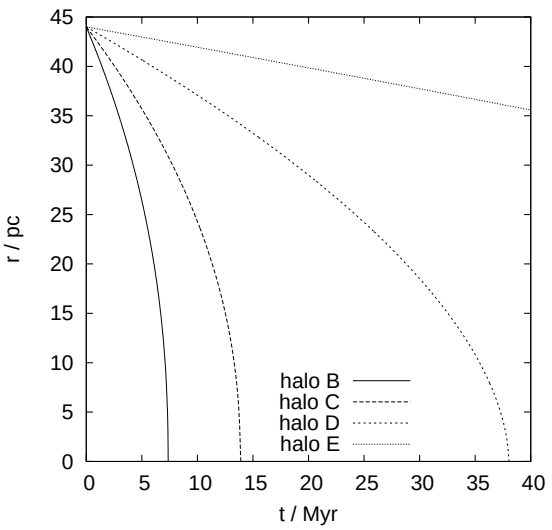

Figure 9. Analytical computed position as a function of time, during the Chandrasekhar sink-in period for four of our haloes, assuming an initial true distance of the nucleus from the centre of 44 pc.

$$P_{\rm n_{dn}>2} = 1 - \sum_{\rm j=0}^{2} \binom{50}{j} (P_{\rm dn})^{\rm j} (1 - P_{\rm dn})^{50-\rm j} \qquad (20)$$

For the values of our halo D we have $P_{\rm n_{dn}>2} = 0.0941\%$ or alternatively $P_{\rm n_{dn}<3} = 99.91\%$. This is valid under the assumption, we made earlier, that the inclination angle i is smaller than 43°. But this assumption holds only in $P_{\rm angle} = 70\%$ of all the cases. Therefore we can exclude halo D with a probability of $P_{\rm angle}^{\rm exclude} = P_{\rm angle} P_{\rm n_{dn}<3} = 69.9\%$.

In order to obtain exclusion probabilities, which are independent of an arbitrarily chosen inclination angle i, one has to integrate the i dependent probability of seeing less than 3 galaxies with double nuclei in the sample $P_{\rm n_{dn}<3}(i)$ over all angles normalised by their probability density:

$$P_{\rm exclude} = \int_0^{\pi/2} \cos(i) P_{\rm n_{dn}<3}(i) {\rm d}i \qquad (21)$$

Table 2 shows those values for the different haloes. A clear trend becomes apparent. The excludability increases with

Halo	γ	$P_{\rm exclude}$
B	1.50	$99.31\% \triangleq 2.70\sigma$
C	1.00	$98.89\% \triangleq 2.54\sigma$
D	0.75	$97.99\% \triangleq 2.32\sigma$
E	0.50	$90.63\% \triangleq 1.68\sigma$

Table 2. Statistical implications of neglecting the cusp-core transformation mechanism explained in §2 for the different halo models derived by our analytical calculations.

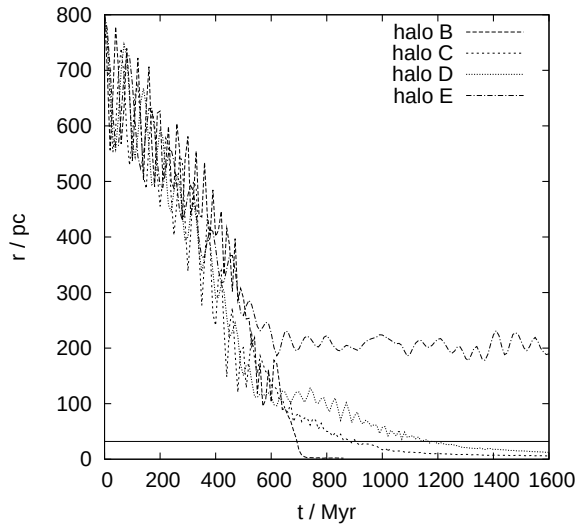

Figure 10. Separation of the two perturbers as a function of time, assuming an initial true separation of 800 pc and perpendicular orbits. The horizontal line shows the observed projected distances in VCC 128.

increasing γ, as we might expect. So there is an upper limit on γ. Looking carefully at the probabilities given in Table 2 we must come to the conclusion that in absence of the cusp-core transforming mechanism described in the last section the inner log density slope of VCC 128 must be extremely shallow.

We ran an additional series of simulations with two perturbers on either coplanar or perpendicular orbits. Again we used the haloes presented in Table 1. The stalling behaviour is shown in Fig. 10. In haloes B, C and D, the nuclei do not stall. Only in halo E do they stall above 32 pc. These results suggest for slopes of 1.0 or steeper, this stalling mechanism does not crucially change the results we derived analytically in this section. However for slopes shallower than 1.0 it affects these results quite dramatically.

To summarise our findings: We can indeed exclude all steep inner log density slopes of 0.75 or higher. The most likely explanation for the observation is however that the two nuclei transformed an initially steeper density profile with an inner log density slope between 0.75 and 0.5 into a core during its initial sinking period. The nuclei would then stall at the edge of this freshly created core. A very shallow inner log density slope like 0.5 or smaller seems to be quite unlikely as well, because the globular clusters would have stalled far further away then 32 pc (at 100 - 200 pc; see Fig. 10). Therefore one can deduce that an underlying dark matter halo with $\gamma \sim 0.75 - 0.5$ at $\sim 1\%$ of the virial radius provides the best explanation for the shown observations. One should note here that this cusp-core transformation mechanism does not explain the dynamical friction timescale problem of Fornax within a ΛCDM ($\gamma = 1.0$) halo (see Fig. 3 of Goerdt et al. (2006)), because in that case the globular clusters in Fornax are far too light and far too distant from the centre of their host galaxy for this cusp-core transformation mechanism to play a significant role. Equation (14) predicts for the halo they are using, assuming $\kappa = 0.441$ for a $\gamma = 1.0$ halo, a core of only 44 pc. This is far smaller then the radius of the innermost globular cluster in Fornax, which is at 240 pc.

4 CONCLUSIONS

A sufficiently compact sinking perturber will transform an initially cuspy host halo into a cored one on some scale. Once a core has formed then dynamical friction is no longer effective (Goerdt et al. 2006). Dynamical arguments show that sinking perturbers must stall at the outer edge of a core (Read et al. 2006).

In this paper we quantify this stalling behaviour as a function of perturber mass and central cusp slope. We give empirical scaling relations using high resolution N-body simulations and attempt to explain these using simple energetic arguments. We describe a mechanism which is capable of transforming primordial cusps into cores. At first sight, this mechanism looks promising for solving the cusp core problem because it naturally explains cores in a ΛCDM universe. From equation (14), a $\sim$1 kpc sized core will form from a single perturber having 1% of the mass of its host (assuming $\kappa = 0.441$ for $\gamma = 1.0$). This essentially recovers the earlier results of El-Zant, Shlosman & Hoffman (2001) and El-Zant et al. (2004). However, we require a *point mass* with 1% of the host mass – that is, for example, a $10^7\,{\rm M}_\odot$ point mass in a $10^9\,{\rm M}_\odot$ dwarf galaxy – which seems unrealistic. But there is a further problem. The effect is strongest only when the mass of the perturber matches the enclosed mass of the host galaxy. Thus, unless the perturber is a black hole, a bright dense nucleus will form making the dark matter dynamically irrelevant. Such galaxies undoubtedly exist, but they are not the typical LSB galaxies for which the cusp-core problem is most famous (de Blok 2005). All of this explains why detailed numerical simulations that model the dissipation of gas and star formation do not see cusps turn into cores, despite the stars being over-concentrated due to over-cooling (Macciò et al. 2006).

Although not necessarily important for the cusp-core problem, the cusp-core transformation mechanism we describe in this paper could explain the abundance (3/50) of dwarf spheroidal galaxies (dSphs) in Virgo with close double nuclei. We focused on the dSph VCC 128 which has a double nucleus of projected separation 32 pc (Debattista et al. 2006). We suggested a new model where the double nucleus is formed by two infalling globular clusters that create a smaller constant density core and then stall. We demonstrated that VCC 128 is likely dark matter dominated and placed constraints on the distribution of dark matter re-

quired for this core-stalling mechanism to be effective. We found that:

- The inner log density slope γ of the dark matter halo of VCC 128 must be less than 0.75 at $\sim 0.1\%$ of the virial radius. For $\gamma > 0.75$ initially, the dynamical friction sink-in time is so small in comparison to the lifetime of the galaxy that we run into a fine tuning problem. For $\gamma < 0.75$ initially, the nuclei create a central constant density core of separation ~ 40 pc after which they stall.
- The initial inner log density slope γ must be greater than 0.5. Otherwise the globular clusters would stall well beyond their current projected separation of 32 pc.

The above may be indirect observational evidence for central dark matter cusp slopes shallower than r^{-1} near the centres of dark matter haloes. Unfortunately, published numerical simulations of CDM halo structure have not quite reached this resolution (Graham et al. 2006), which requires following over a billion particles within the final halo.

ACKNOWLEDGEMENTS

It is a pleasure to thank Ioannis Sideris and Eyal Neistein for carefully reading the manuscript. For all N-body simulations we used PKDGRAV2 (Stadel 2001), a multi-stepping tree code developed by Joachim Stadel. All computations were made on the zBox2 supercomputer at the University of Zürich. Special thanks go to Doug Potter for bringing it to life. Tobias Goerdt is a Minerva fellow.

REFERENCES

Calcáneo-Roldán C, Moore B, 2000, Phys. Rev. D, 62, 123005
Capuzzo-Dolcetta R, Vicari A, 2005, MNRAS, 356, 899
Chandrasekhar S, 1943, ApJ, 97, 255
Colpi M, Mayer L, Governato F, 1999, ApJ, 525, 720
Debattista V. P, Ferreras I, Pasquali A, Seth A, de Rijke S, Morelli L, 2006, ApJ, 651, 97
de Blok W. J. G, 2005, ApJ, 634, 227
de Rijcke S, Michielsen D, Dejonghe H, Zeilinger W. W, Hau G. K. T, 2005, A&A, 438, 491
Diemand J, Moore B, Stadel J, 2005, Nature, 433, 389
Dubinski J, Carlberg R. G, 1991, ApJ, 378, 496
El-Zant A, Hoffman Y, Primack J, Combes F, Shlosman I, 2004, ApJ, 607, 75
El-Zant A, Shlossman I, Hoffman Y, 2001, ApJ 560, 636
Ferrarese L, 2002, ApJ, 578, 90
Ferrarese L, Côté P, Dalla Bontà E. et al, 2006, ApJL, 644, 21
Goerdt T, Gnedin O. Y, Moore B, Diemand J, Stadel J, 2007, MNRAS, 375, 191
Goerdt T, Moore B, Kazantzidis S, Kaufmann T, Macciò A. V, Stadel J, 2008, MNRAS, 385, 2136
Goerdt T, Moore B, Read J. I, Stadel J, Zemp M, 2006, MNRAS, 368, 1073
Graham A. W, Driver S. P, 2005, PASA, 22, 118
Graham A. W, Merritt D, Moore B, Diemand J, Terzić B, 2006, AJ, 132, 2701
Gualandris A, Merritt D, 2008, ApJ, 678, 780
Hernquist L, 1990, ApJ, 356, 359
Hernquist L, Weinberg M. D, 1989, MNRAS, 238, 407
Kalnajs, A. J, 1972, in Lecar M, ed, Proc. IAU Colloq. 10, Gravitational N-Body Problem, Reidel, Dodrecht
Kazantzidis S, Magorrian J, Moore B, 2004, ApJ, 601, 37
Kleyna J. T, Wilkinson M. I, Gilmore G, Evans N. W, 2003, ApJ, 588, 21, Erratum-ibid, 2003, 589, 59
Koushiappas S. M, 2006, Phys. Rev. Lett, 97, 191301
Lauer T. R. et al, 1996, ApJ, 471, 79
Lin D. N. C, Tremaine S, 1983, ApJ, 264, 364
Łokas E. L, 2002, MNRAS, 333, 697
Lotz J. M, Miller B. W, Ferguson H. C, 2004, ApJ, 613, 262
Macciò A. V, Moore B, Stadel J, Diemand J, 2006, MNRAS, 366, 1529
Moore B, 1994, Nature, 370, 629
Peñarrubia J, Just A, Kroupa P, 2004, MNRAS, 349, 747
Read J. I, Goerdt T, Moore B, Pontzen A. P, Stadel J, Lake G, 2006, MNRAS, 373, 1451
Read J. I, Trentham N, 2005, RSPTA, 363, 2693
Saha P, 1992, MNRAS, 254, 132
Sánchez-Salcedo F. J, Reyes-Iturbide J, Hernandez X, 2006, MNRAS, 370, 1829
Stadel J, 2001, PhD thesis, Univ. Washington
Tonini C, Lapi A, Salucci P, 2006, ApJ, 649, 591
Tremaine S, 1995, AJ, 110, 628
Tremaine S, Weinberg M. D, 1984, MNRAS, 209, 729
Wehner E. H, Harris W. E, 2006, ApJL, 644, 17
White S. D. M, 1983, ApJ, 274, 53
Zemp M, Moore B, Stadel J, Carollo C. M, Madau P, 2008, MNRAS, 386, 1543
Zhao H, 1996, MNRAS, 278, 488